PCCP

Accepted Manuscript




ROYAL SOCIETY OF CHEMISTRY

www.rsc.org/pccp

# Charge-Induced Equilibrium Dynamics and Structure at the Ag (001) – Electrolyte Interface

Robert M. Karl Jr.[1◊], Andi Barbour[2◊], Vladimir Komanicky[3], Chenhui Zhu[2], Alec Sandy[4], Michael S. Pierce[1*], and Hoydoo You[2 *]

[1]*School of Physics and Astronomy, Rochester Institute of Technology, Rochester NY, 14623, USA*

[2]*Materials Science Division, Argonne National Laboratory, Argonne IL 60439, USA*

[3]*Faculty of Science, Safarik University, 04001Košice, Slovakia*

[4]*Advanced Photon Source, Argonne National Laboratory, Argonne IL 60439, USA*

The applied potential dependent rate of atomic step motion of the Ag (001) surface in weak NaF electrolyte has been measured using a new extension of the technique of X-ray Photon Correlation Spectroscopy (XPCS). For applied potentials between hydrogen evolution and oxidation the surface configuration completely changes on timescales of $10^2$ - $10^4$ seconds depending upon the applied potential. These dynamics, directly measured over large areas of the sample surface simultaneously, are related to the surface energy relative to over or under potential. Concurrent specular x-ray scattering measurements reveal how the ordering of the water layers at the interface correlates with the dynamics.

**Keywords:** X-ray Photon Correlation Spectroscopy, Surface X-ray Scattering, Water-Metal Interface

---

◊ Author contributed equally to manuscript

◊ Author contributed equally to manuscript

* Hoydoo You: you@anl.gov

* Michael S. Pierce: mspsps@rit.edu.

Knowledge of the behavior of ions and molecules at surfaces and interfaces is vital to many fundamental and technological processes, such as electro-catalysis, corrosion, device fabrication, and mono-layer self assembly. New techniques for the study of surfaces continue to be developed, such as *in-situ* electrochemical scanning tunneling microscopy [1, 2], *in-situ* surface x-ray scattering [3, 4, 5, 6], and x-ray phase contrast microscopy [7]. One key aspect of surface science, which contains significant gaps, is direct observation of the dynamic behavior of surfaces and interfaces in such environments. Although the dynamics of surfaces under high and low vacuum have been studied using conventional surface science tools [8], these same interfaces under real-world conditions are significantly less studied and not as well understood. One critically important area in this realm is electrochemically active interfaces in acidic or basic solutions. Due in part to a lack of dynamics data, empirical observations of these systems are generally far beyond basic, first-principle understanding.

The adsorption and reactivity of supported nano-particles [9, 10] and extended surfaces have both received a great deal of attention for their applications in heterogeneous catalysis and catalytic converters. Surfaces such as Ag, Pt, and Au crystals are model catalysts and have proved rich in character for both experimental [11, 12, 13, 14] and theoretical study [15, 16, 17, 18]. The wide variety of acidic and basic electrolyte with and without additives such as halides [19, 20, 21], metal adsorption and deposition [22, 23, 24, 25], and temperature effects [26, 27] have made these some of most important surface systems studied to date.

Measurements of model catalyst or electrode surfaces, such as single crystal facets of precious metals, can provide insight into the physical and chemical character of these simplified systems. The Ag (001) surface represents just such a system, having been extensively studied using conventional surface techniques. There are beautiful examples of layer growth in Ag [28], as well as experiments showing the onset of oxide layer formation for potentials above PZC [29]. However, such earlier measurements are largely lacking for details of the surface evolution of nano-scale features such as atomic terraces and islands, over large length scales, and utilizing extensive *in-situ* measurement over a wide range of electric potentials. To address these issues, using a combination of surface x-ray scattering techniques, the structure and evolution of Ag (001) in 0.02 M NaF electrolyte was measured as a function of applied potential.

X-ray Photon Correlation Spectroscopy (XPCS) is the extension of laser Dynamic Light Scattering to x-ray wavelengths. This technique has found wide application, with great success at measuring the dynamics of polymers, liquid crystal interfaces, magnetic domains, and martensites, among many other systems [30]. XPCS at surfaces and interfaces has a rich history of success in measuring the dynamics occurring at interfaces [31, 32] and is itself an established field [33, 34]. However, it was only recently that coherent surface x-ray scattering and XPCS was extended to study surfaces with atomic terrace and surface monolayer sensitivity [35, 36], due in large part to increased flux from modern synchrotron x-ray sources. These experiments provide an ensemble average

of the surface state over large areas of the interface. However, while experiments conducted in vacuum environment have lent themselves to good interpretation [37], more complicated surfaces, such as the electrolyte – catalysts interface, have proven difficult to firmly describe [36]. Coherent x-ray scattering from surfaces is sensitive to the precise arrangement of surface structures, step edge terraces, and islands, and can be used to determine the rate of evolution under different conditions and potentials. In this respect Ag (001) in weak NaF solution surface is superior to Au or Pt as it does not possess a surface reconstruction. Hence the dynamics observed can be directly ascribed to the motion of step edges. In these experiments relatively length scales corresponding to atomic thicknesses were probed. Timescales of several $10^4$ s were obtained in regions of slow, essentially static evolution, while rapid changes on time scales of several 10 s to 100 s were observed when the surface was rapidly evolving.

Likewise, direct structural information was obtained from specular crystal truncation rod measurements which capture the vertical electron density profile along the normal to the surface-electrolyte interface. These indicate that at some ranges of applied potentials ordered water layers are present above the Ag (001) surface, similar to earlier studies of the Ag (111) – electrolyte surface [3, 38, 39]. The limited out of plane ordering of liquid water exposure at room temperature contrasts well with highly controlled UHV low temperature water studies of the Ag (001) surface which indicate full 3D crystalline growth [40].

These experiments were conducted at the Advanced Photon Source at Argonne National Laboratory using the 8-ID-E beamline [41] and the large angle XPCS station. A Si (111) single bounce monochromator was used to select photons with an energy of 7.35 keV and a bandwidth of $10^{-4}$. The incident radiation was then vertically focused to 3 μm using a kinoform lens and precision slits were used to narrow the beam to 10 μm in the horizontal direction. This resulted in a highly coherent flux of ~ 2 x $10^9$ photons/sec. Due to the relatively small optical path length differences obtained through surface scattering, the longitudinal coherence provided by the single bounce monochromator was sufficient even when sample geometry projected the beam over a large area. A low noise Princeton Instruments x-ray CCD was used to detect the scattered photons, with typical image exposures of 1-2 s. The slit to sample distance was 215 mm and the sample to detector distance was 1.0 m, which nominally places the speckle dimensions at just over the 20 x 20 μm pixel size of the detector. During the experiments purposeful offset translations of the sample laterally showed no effect on decorrelation rates, confirming a true ensemble measurement of the surface. Long timescale measurements in static conditions, with autocorrelation decays of several $10^4$ s, up to $10^5$ s, confirmed the overall stability and integrity of the experiment in static conditions.

The Ag (001) crystal was cleaned in acetone prior to being bulk annealed using a radio frequency (RF) induction heater overnight in Ar/H flow at 850 ºC. Surface annealing just before experiment was done for 15

minutes at the same conditions. A droplet of ultrapure water (Mili-Q, resistivity 18 MOhm.cm) was placed over the crystal after cooling to protect from air-born contamination. The crystal was then mounted in the x-ray cell and placed on the goniometer. The electrolyte solution was produced from Sigma-Aldrich BioXtra grade NaF reagent with an assay of less than 100 ppm sulfate and less than 10 ppm chloride. Weakly interacting concentrations of 0.02 M NaF were typically used, with additional tests at 0.002 M showing no quantifiable deviation in results.

In order to determine the rate of surface evolution, the second order autocorrelation $g_2$ was calculated using a symmetric normalization scheme. The calculations were performed using both the available XPCSGUI analysis package as well as custom written routines. The background subtracted autocorrelation was calculated on a pixel by pixel basis according to

$$g_2(\Delta t) = \langle I(t+\Delta t)I(t)\rangle / \langle I(t+\Delta t)\rangle\langle I(t)\rangle \qquad (1)$$

The resulting autocorrelation data is then related to the intermediate scattering function $f(\boldsymbol{q}, \Delta t)$ through

$$g_2(\Delta t) = \beta |f(\boldsymbol{q}, \Delta t)|^2 + 1 = \beta e^{-\Delta t/\tau} + 1 \qquad (2)$$

where $\beta$ is the contrast of the speckle pattern, and $\tau$ is the decay constant of the autocorrelation. For these measurements no stretching or compression exponent was needed, nor were multiple timescales observed during equilibrium measurements. Representative examples of the autocorrelation data and accompanying fits are shown in Figure 1. Additionally two-time correlation analysis and centroid tracking were conducted prior to the full autocorrelation calculation to provide independent verification of speckle evolution and quality. The two-time analysis computes the product of a speckle with itself, with the diagonal representing a $\Delta t$ of zero. Variation in the decorrelation rate, be it gradual or abrupt, will be readily evident as a feature in the two-time plot. An example two-time correlation map is in the inset of Fig.1 showing rapid equilibrium evolution observed at -1.1 V. Only regions of sufficiently stable evolution would then be used to calculate the autocorrelations. Centroid tracking provides confirmation of the static nature of the overall scattering envelope, eliminating false decorrelation due to motion.

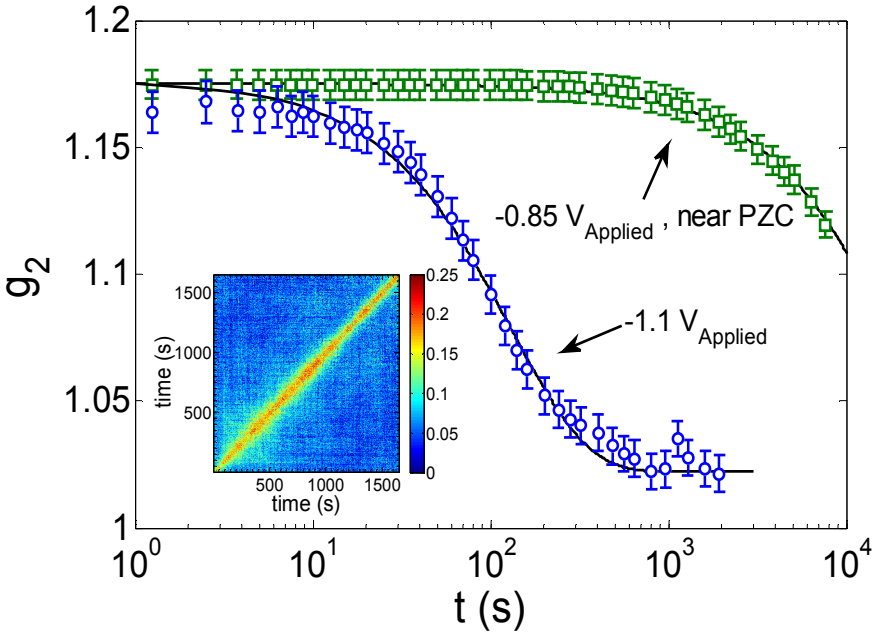


FIG. 1. Shown are two example autocorrelation functions at different applied potentials. The rate of change near PZC is significantly slower than what is observed at -1.1V. Inset: two-time correlation map for -0.6V. The width of the central band is related to the decorrelaton rate of the dynamics.

Measurements were collected while holding the potential constant for periods of time sufficient for equilibrium conditions to be reached, typically staying at a single potential for 0.5-2 hours. The potential would then be changed and data collected as the system relaxes to a new equilibrium condition. The primary modes of data acquisition were to slowly take the sample around the current-potential loop in the range between oxide formation and hydrogen evolution, as well as starting from PZC and proceeding in each direction. The XPCS measurements reported here were collected at the reciprocal space location (0,0,0.17) as a compromise between surface sensitivity and signal. Similar to earlier XPCS studies of Au in perchloric acid [36], no statistically meaningful direct q-dependence was observed within a single scattering envelope of an image. As such, the correlations from the regions of semi-uniform scattering intensity were averaged to maximize signal.

The time constants shown in Figure 2 were observed by starting from PZC and then slowly moving to potentials away from PZC. For potentials near PZC the time constants are large ~ $10^4$ sec. As the potential is varied away from PZC the time constants decrease quickly, dropping to values as low as ~ $10^2$ sec, achieving full decorrelation and sustained equilibrium conditions for hours as seen in the inset plot in Fig. 2. Eventually once the potential is relatively far from PZC, the surface approaches the hydrogen evolution region on cathodic side, or

nears oxidation potential when sufficiently positive; in both cases a sudden slowing of the surface evolution is observed.

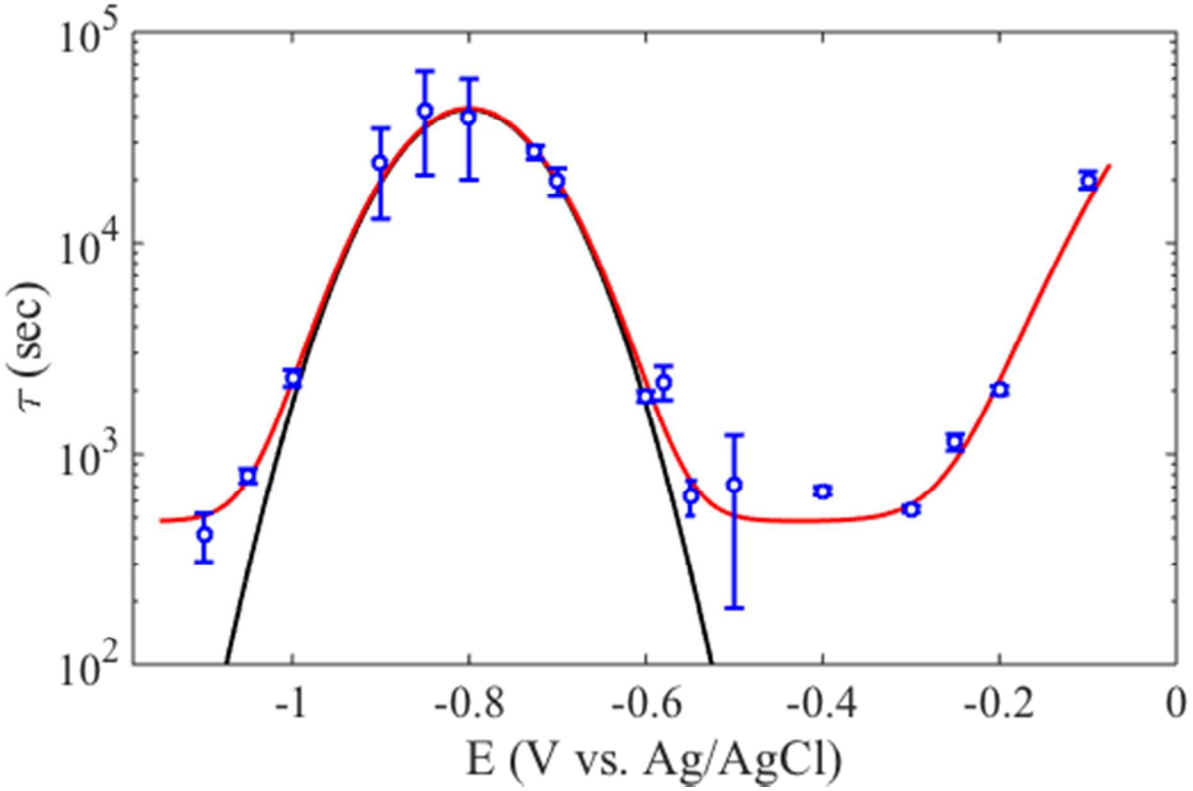


FIG. 2. (Color online) Decay constant as a function of applied potential at (0,0,0.17). The solid black line corresponds to only the contribution from Eq. 3, while the dashed red line includes the phenomenological component. For reference, PZC is near -0.8 V.

This behavior can be modeled by the ansatz that the dynamics should be related to the surface tension (energy) present at the interface. As the 0.02 M NaF electrolyte is relatively weakly interacting, no mass transport should be occurring at the surface. Additionally, the XPCS signal is most sensitive to motion of the surface steps. Hence it is possible to measure the step edge contribution to the overall capacitance of the interface [42, 43]. Given these assumptions, the inverse of the time constants could be expected to follow a simple relation of

$$\tau^{-1} \propto e^{\{-E_A + C\eta^2/2\}/k_B T} \qquad (3)$$

where $E_a$ represents an activation barrier energy for step motion to occur in the absence of any potential, $\eta = V - V_{PZC}$ gives the relative amount of under or over-potential, and C represents the capacitance at the step edges. An additional phenomenological piece can be added to describe the behavior of the time constants far from PZC and thus fixing the relative evolution rate as a function of applied potential. Since the q-dependence of the data points is the same for each potential, this overall effect can then be factored out leaving the activation energy in Eq. 3 intact. Ex-situ voltammetry determined $V_{PZC}$ = 0.80 V(vs. Ag/AgCl). The resulting fit using the remaining parameters is shown in Fig. 2. The activation barrier is then 0.19 (0.02) eV and represents how difficult it is for random step motion to occur in the absence of an applied potential. This value compares positively with the energy barrier expected from an Ag atom at a kink on a step edge [44, 45] and also to diffusion studies at the Ag (111) interface [46]. The step capacitance parameter is 0.44 (.07) mF/cm$^2$. This corresponds to the capacitance for a surface dominated by step edges. Given the small miscut of the sample surface, the contribution of the step edges to the total capacitance would be much smaller. At potentials far from PZC the surface evolution slows. This is likely due to the pinning of surface features due to the approach of surface oxidation or hydrogen evolution regions. To account for this a phenomenological term can be added to describe the amount of oxidation at a given potential

Non-equilibrium dynamics were mostly seen after a change in applied potential, usually stabilizing within a few tens of minutes or less. The non-equilibrium dynamics typically consisted of the decorrelation rate changing steadily after a change in potential. An example of this can be seen in the two-time correlation plot in Fig. 1 at early times. However, avalanche type dynamics [30, 47] were also observed in some instances in as a response to an unstable configuration after a change in potential. Such behavior indicates the surface configuration becoming locked in an unfavorable condition that eventually relaxes in a sudden fashion.

Additionally, XPCS data was also collected during IV cycling of the sample. Measurement of the average intensity, hence surface ordering, as a function of applied potential is a useful measurement in many electrochemical systems [4]. Here, the average intensity was found to cyclically repeat with slow variation of applied potential at ~ 2.5 mV/sec over the range of -1.2 V to -0.1 V. An example of the intensity along one cycle is shown in the top panel of Fig. 3. In contrast, a correlation coefficient [48] measuring the degree of correlation between image pairs is observed to monotonically decrease during IV cycling. This decay happens at a faster rate than if the sample were merely sitting at equilibrium conditions. As shown in bottom of Fig. 3, within four cycles the surface has no remaining correlation. Furthermore, it is important to note that there is no evidence of any return in the speckle patterns by the comparison of correlations after ½ cycles and those calculated after full cycles. If there were any memory effect present in the microstate of the surface, it is expected that the correlation

coefficient would recover to some extent when comparing correlations at half cycles to subsequent whole cycle correlations. As such, it can be concluded that the evolution of the surface is not restrained by static defects or pinning sites to a measureable extent, and the configuration of surface steps, terraces, and islands does not repeat during the cycling process as has been observed in speckle measurements of hysteretic systems [49].

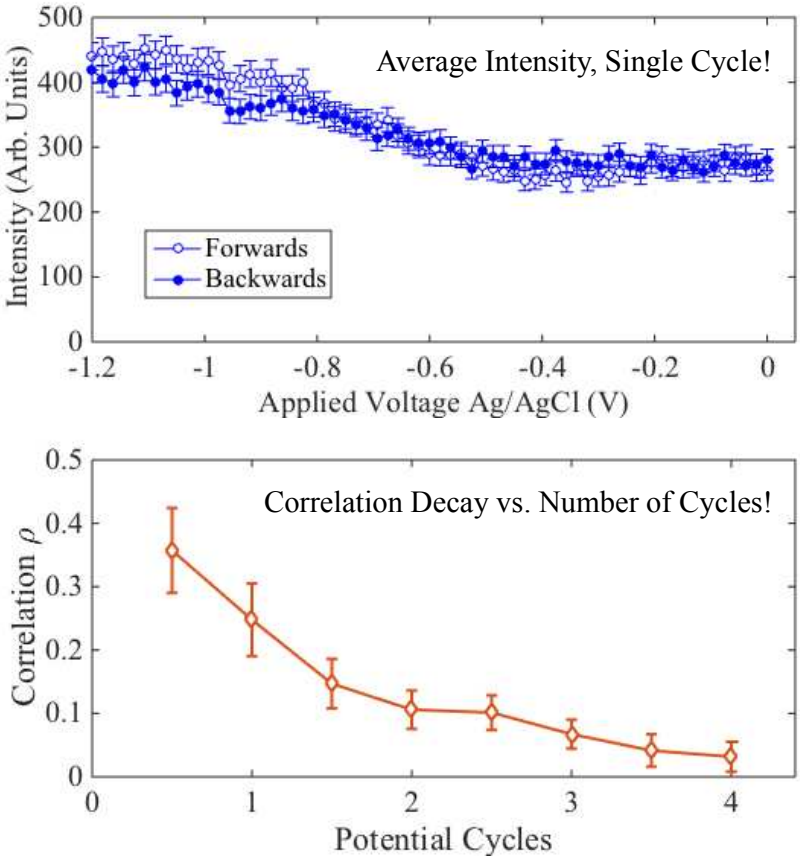


FIG. 3. Top: The average intensity at (0,0,1.05) while the potential is slowly being changed between -1.2 and 0 V. The intensity repeats with each cycle. Bottom: The correlation coefficient as a function of cycles. The rate of decay is faster than would be observed for equilibrium dynamics and also shows no evidence of repetition.

To accompany the coherent x-ray scattering studies, a series of specular crystal truncation rod (CTR) measurements [50, 51] were conducted at four constant potentials through the 2nd Brillouin zone during the same cycles as the XPCS experiments. The observed scattering is similar to measurements conducted of the Ag (111) surface [11, 12]. A simple surface profile, allowing for the possibility of ordered water layers at the interface, was used to fit the observed data [52]. The functional form of the contribution from the water to the overall scattering amplitude is given by

$$f_{water}(q) \propto \frac{e^{-\frac{q^2\sigma_0^2}{2}+iqd_0}}{1-e^{-\frac{q^2\bar{\sigma}^2}{2}+iqd_w}} \qquad (4)$$

where $d_0$ is the displacement of the water above the interface, $d_w$ is the subsequent spacing of the water layers, $\sigma_0$ is related to the width of the water layers, and $\bar{\sigma}$ is related to the dampening of the layers. Once the initial parameter set was established, fixing parameters such as the Debye Waller factor and the ratio of sample to diffuse water electron density, only the 4 specific ordering parameters from Eq. (4) were allowed to vary between fits at different potentials. A subset of the data shown in Fig. 4 is the specular scattering at -1.1 V and -0.25 V. While Eq. 4 provides an over-simplification of the electrolyte – Ag interface, adjusting the model to include additional parameters does not make for a statistically more meaningful fit.

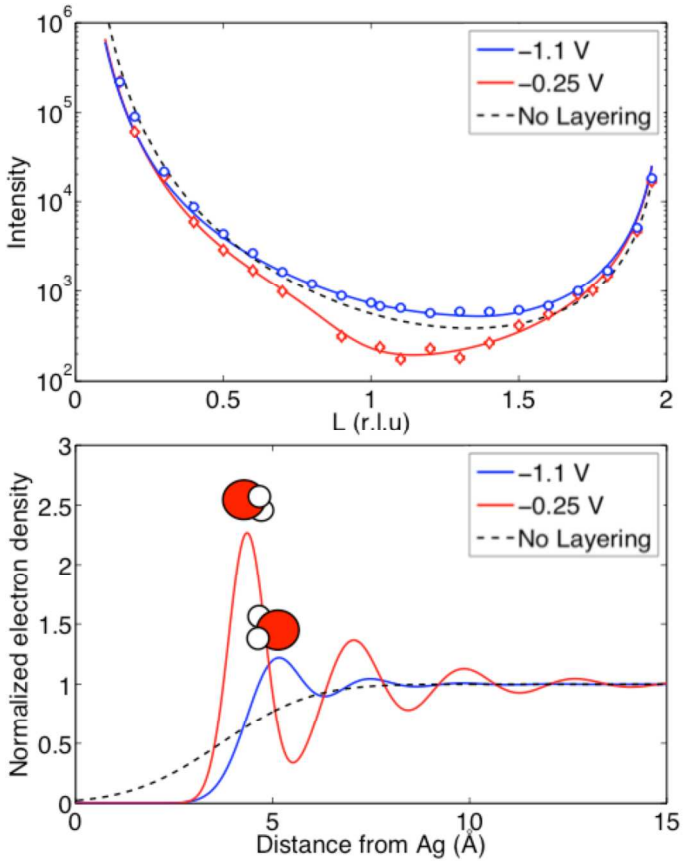


FIG. 4. (Color online) Top: A portion of the CTR data for Ag (001) at two applied potentials. Bottom: Fitting these extracts the structure of water near the crystal surface. Included in each is a dashed line showing the effect of turning off the water layering.

The ordered layers result in destructive interference and an intensity drop. The resulting fits are consistent with ordered water layering at the interface. The distance to the first layer varies directly with the applied potential. This potential dependent behavior of $d_0$ is consistent with relative dipole orientation shifting for the each side of PZC [11, 12]. The electron density profiles are shown in Fig. 4. The -1.1 V data shows a significant decrease to the water ordering. While this represents the first measurement of ordered water layers at the Ag (001) – water surface, the more significant observation comes from the relation of the water ordering to the observed dynamics. The ordered layers only reside over the interface configurations with relatively slow evolution. In the case of the -1.1 V potential, the surface may be too unstable and dynamic to allow for a significant ordering at the interface. Included in Fig. 4 is a dashed line showing the result of removing the water layering at the interface.

The fit parameters from the structural analysis are plotted vs. $\tau$ in Fig. 5. The dampening of the layers $\bar{\sigma}$ increased with increasing $\tau$; this corresponds to the water layering becoming more pronounced for slower dynamics. The peak width parameter $\sigma_0$, which also corresponds to the inverse of the peak height, decreased with increasing $\tau$, indicating that the water is more ordered when the dynamics are slower. It is not likely the dynamics of the surface features itself that drives relative change in interfacial ordering. Rather both are likely the result of the impact of local surface energy and surface tension on the structure and dynamics.

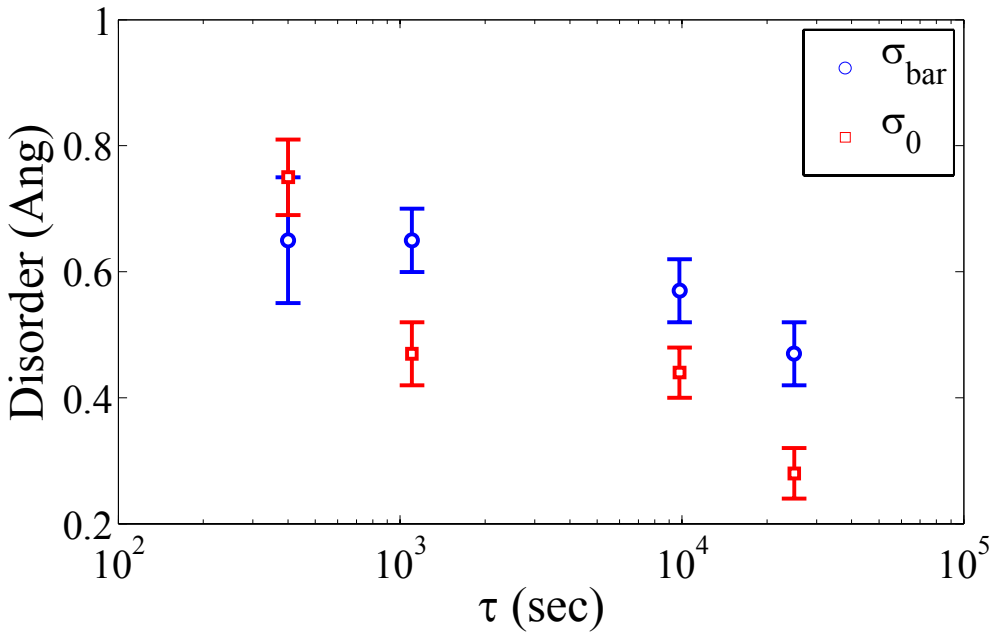


FIG. 5. (Color online) Fit parameters as a function of time constant. $1/\sigma_0$ corresponds to the peak width while $\bar{\sigma}$ corresponds to the dampening of the peaks. Decreasing $\sigma_0$ and $\bar{\sigma}$ both correspond to a more prominent layering, which is observed for longer time constants.

These x-ray scattering experiments represent the first direct ensemble averaged measurement of the rate of surface changes to the Ag (001) surface in electrolyte. For applied potentials between hydrogen evolution and oxidation the surface configuration completely changes on timescales of 100 s - $10^4$ seconds depending upon the applied potential. These dynamics, directly measured over large areas of the sample surface simultaneously, are related to the surface energy relative to over or under potential. For dynamics occurring near the PZC there is a potential dependent effect due to the step-line capacitance and a slow evolution due to atoms diffusing from kinks and step edges. During the same experiment specular x-ray scattering was used to measure the average ordering of the Ag (001) – electrolyte interface. The relative surface ordering was found to vary directly with the rate of surface evolution observed in the XPCS measurements. The experiments demonstrate a limited out of plane ordering of water molecules at room temperature when exposed to liquid water. Additionally, this set of measurements is the first ever combination of XPCS and CTR experiments within a single system and demonstrates the potential such combined studies.

This work and the use of the Advanced Photon Source were supported by the US Department of Energy, Office of Basic Energy Sciences, under Contract No. DE-AC02-06CH11357. The work at Safarik University was supported by Slovak Grant No. VEGA 1/0782/12. Data analysis was conducted using the Large Memory Computer system available through the RIT Research Computing facilities. The authors wish to thank Junghune Nam and Suresh Narayanan for their assistance with the experiments at 8ID of the APS, and Yihua Liu for many useful discussions.

[1] X. Gao, A. Hamelin, and M.J. Weaver, Phys. Rev. Lett. **67**, 618 (1991).

[2] O.M. Magnussen, Chem. Rev. **102**, 679 (2002).

[3] M.F. Toney, J.G. Gordon, M.G. Samant, G.L. Borges, O.R. Melroy, L-S Kau, D.G. Wiesler, D. Yee, and L.B. Sorensen, Phys. Rev. B **42**, 5594 (1990).

[4] B.M. Ocko, J. Wang, A. Davenport, and H. Isaacs, Phys. Rev. Lett. **65**, 1466 (1990).

[5] Z. Nagy and H. You, Electrochimica Acta **47**, 3037 (2002).

[6] F. Golks, K. Krug, Y. Gruender, J. Zegenhagen, J. Stettner, and O.M. Magnussen, J. Am. Chem. Soc. **133**, 3772 (2011).

[7] P. Fenter, C. Park, Z. Zhang, and Steve Wang, Nature Physics **2**, 700 (2006).

[8] A. Hodgson and S. Haq, Surface Science Reports **64**, 381 (2009).

[9] M. Haruta, Catalysis Today **36**, 153-166 (1997).

[10] M. Valden, X. Lai, and D.W. Goodman, Science **281**, 1647-1650 (1998).

[11] M.F. Toney, J.N. Howard, J. Richer, G.L. Borges, J.G. Gorgon, O.R. Melroy, D.G. Wiesler, D. Yee, and L.B. Sorensen, Nature **368**, 444-446 (1994).

[12] M.F. Toney, J.N. Howard, J. Richer, G.L. Borges, J.G. Gordon, O.R. Melroy, D.G. Wiesler, D. Yee, and L.B. Sorensen, Surface Science **335**, 326-332 (1995).

[13] B.M. Jovic', V.D. Jovic', and G.R. Stafford, Electrochemistry Communications **1**, 247 (1999).

[14] S-G Sun, W.-B. Cai, L.-J. Wan, and M. Osawa, J. Phys. Chem. B **103**, 2460-2466 (1999).

[15] K.-P. Bohnen and K.M. Ho, Electrochimica Acta, **40**, 129-132 (1994).

[16] T. Jacob, Electrochimica Acta **52**, 2229-2235 (2007).

[17] H-Y Su, M-M Yang, X-H Bao, and W-X Li, J. Phys. Chem C **112**, 17303-17310 (2008).

[18] Y.J. Feng, K.P. Bohnen, and C.T. Chan, Phys. Rev. B **72**, 125401-8 (2005).

[19] O. Endo, M. Kiguchi, T. Yokoyama, M. Ito, T. Ohta, J. of Electroanalytical Chemistry **473**, 19-24 (1999).

[20] D.D. Sneddon, A.A. Gewirth, Surface Science **343**, 185-200 (1995).

[21] T. Wandlowski, J.X. Wang, and B.M. Ocko, J. Electroanalytical Chemistry **500**, 418-434 (2001).

[22] V.D. Jovic', B.M. Jovic', and A.R. Despic', J. Electroanalytical Chemistry **288**, 229-243 (1990).

[23] H. Siegenthaler, K. Juettner, E. Schmidt, and W.J. Lorenz, Electrochimica Acta **23**, 1009-1018 (1978).

[24] K.J. Stevenson, D. W. Hatchett, and H.S. White, Langmuir **12**, 494-499 (1996).

[25] J.X. Wang, R.R. Adzic', O.M. Magnussen, and B.M. Ocko, Surface Science **344**, 111-121 (1995).

[26] A. Hamelin, L. Doubova, L. Stoicovicio, and S. Trasatti, J. Electroanalytical Chemistry **244**, 133-145 (1988).

[27] C.A. Lucas, P. Thompson, M. Cormack, A. Brownrigg, B. Fowler, D. Strmcnik, V. Stamenkovic, J. Greeley, A. Menzel, H. You, and N.M. Markovic' J. Am. Chem. Soc. **131**, 7654-7661 (2009).

[28] E. Budevskii, V. Bostanov, T. Vitanov, Z. Stoinov, A. Kotseva, and R. Kaishev, Elektrokhimiya **3**, 856 (1967).

[29] Sh.K. Shaikhutdinov, E.R. Savinova, A. Scheybal, K. Doblhofer, and R. Schloegl, Journal of Electroanalytical Chemistry **500**, 208 (2001).

[30] Oleg Shpyrko, Journal of Synchrotron Radiation **21**, 1057-1064 (2014).

[31] J.L. Libbert, R. Pindak, S.B. Dierker, and I.K. Robinson, Phys. Rev. B **56**, 6454-6457 (1997).

[32] H. J. Kim, A. Ruhm, L. B. Lurio, J. K. Basu, J. Lal, D. Lumma, S. G. J. Mochrie and S. K. Sinha, Phys. Rev. Lett. **90**, 068302 (2003).

[33] Sunil K. Sinha, Zhang Jiang, and Laurence B. Lurio, Advanced Materials **26**, 7764-7785 (2014).

[34] Luigi Cristofolini, Current Opinion in Colloid and Interface Science **19**, 228-241 (2014).

[35] M.S. Pierce, K.C. Chang, D. Hennessy, V. Komanicky, M. Sprung, A. Sandy, and H. You, Physical Review Letters **103**, 165501 (2009).

[36] M.S. Pierce, V. Komanicky, A. Barbour, D.C. Hennessy, C. Zhu, A. Sandy, and H. You, Physical Review B **86**, 085410 (2012).

[37] M.S. Pierce, K.C. Chang, D. Hennessy, V. Komanicky, J. Strzalka, A. Sandy, A. Barbour, and Hoydoo You, App. Phys. Lett. **99**, 121910 (2011).

[38] M.F. Toney, J.N. Howard, J. Richer, G.L. Borges, J.G. Gordon, O.R. Melroy, D.G. Wiesler, D. Yee, and L.B. Sorensen, Nature **368**, 444 (1994).

[39] M.F. Toney, J.N. Howard, J. Richer, G.L. Borges, J.G. Gordon, O.R. Melroy, D.G. Wiesler, D. Yee, and L.B. Sorensen, Surface Science **335**, 326 (1995).

[40] H. Ibach, Surface Science **606**, 1534 (2012).

[41] While there is no direct publication related to the large angle XPCS station at 8-ID-E, many of the details of the beamline and hutch can be found in Zhang Jiang, Xuefa Li, Joseph Strzalka, Michael Sprung, Tao Sun, Alec R. Sandy, Suresh Narayanan, Dong Ryeol Lee, and Jin Wang, Journal of Synchrotron Radiation **19**, 627-636 (2012).

[42] Harald Ibach, Margret Giesen, and Wolfgang Schmickler, J. Electroanalytical Chemistry **544**, 13-23 (2003).

[43] G. Valette, J. Electroanal. Chem., **138** 37-54 (1982).

[44] M. Poensgen, J.F. Wolf, J. Frohn, M. Giesen, and H. Ibach, Surface Science **274**, 430-440 (1992).

[45] R.C. Nelson, T.L. Einstein, S.V. Khare, and P.J. Rous, Surface Science **295**, 462-484 (1992).

[46] John D. Porter and Timothy O. Robinson, J. Phys. Chem **97**, 6696-6709 (1993).

[47] Christopher Sandborn, Karl F. Ludwig, Michael C. Rogers, and Mark Sutton, Physical Review Letters **107**, 015702 (2012).

[48] M.S. Pierce, C.R. Buechler, L.B. Sorensen, S.D. Kevan, E.A. Jagla, J.M. Deutsch, T. Mai, O. Narayan, J.E. Davies, K. Liu, H.G. Katgraber, O. Hellwig, E.E. Fullerton, P. Fischer, and J.B. Kortright, Physical Review B **75**, 144406 (2007).

[49] M.S. Pierce, C.R. Buechler, L.B. Sorensen, J.J. Turner, S.D. Kevan, E.A. Jagla, J.M. Deutsch, T. Mai, O. Narayan, J.E. Davies, K. Liu, J. Hunter Dunn, K.M. Chesnel, J.B. Kortright, O. Hellwig, and E.E. Fullerton, Physical Review Letters **94**, 017202 (2005).

[50] I.K. Robinson and D.J. Tweet, Rep. Prog. Phys. **55**, 599-651 (1992).

[51] I.K. Robinson, Phys. Rev. Lett. **50**, 1145 (1983).

[52] P. Fenter and N.C. Sturchio, Progress in Surface Science **77**, 171-258 (2004).